

# Lattice determination of the Batalin-Vilkovisky function and the strong running interaction

A. C. Aguilar<sup>a</sup>, N. Brito<sup>b,c</sup>, M. N. Ferreira<sup>d</sup>, J. Papavassiliou<sup>d</sup>, O. Oliveira<sup>b</sup>, P. J. Silva<sup>b</sup>

<sup>a</sup> University of Campinas - UNICAMP, Institute of Physics Gleb Wataghin, 13083-859 Campinas, São Paulo, Brazil

<sup>b</sup> CFisUC, Department of Physics, University of Coimbra, Coimbra, 3004-516, Portugal

<sup>c</sup> Centre for Mathematical Sciences, University of Plymouth, Plymouth, PL4 8AA, United Kingdom

<sup>d</sup> Department of Theoretical Physics and IFIC, University of Valencia and CSIC, E-46100, Valencia, Spain

---

## Abstract

The Batalin-Vilkovisky function is a central component in the modern formulation of the background field method and the physical applications derived from it. In the present work we report on novel lattice results for this particular quantity, obtained by capitalizing on its equality with the Kugo-Ojima function in the Landau gauge. The results of the lattice simulation are in very good agreement with the predictions derived from a continuum analysis based on the corresponding Schwinger-Dyson equations. In addition, we show that an important relation connecting this function with the ghost propagator is fulfilled rather accurately. With the aid of these results, we carry out the first completely lattice-based determination of the process-independent strong running interaction, employed in a variety of phenomenological studies.

**Keywords:** Lattice QCD, Background Field Method, Schwinger-Dyson equations, strong running interaction,

---

## 1. Introduction

The background field method (BFM) is a powerful framework that permits the implementation of the gauge-fixing procedure necessary for quantizing gauge theories without losing explicit gauge invariance [1–10]. The formulation of non-Abelian gauge theories within this quantization scheme affords a plethora of advantages, both from the formal as well as the practical points of view. Thus, in addition to streamlining a variety of demonstrations related to renormalization, it allows one to tackle efficiently longstanding challenges, such as the gauge-invariant truncation of the Schwinger-Dyson equations (SDEs) [11–17] or the definition of physically meaningful renormalization-group invariant (RGI) quantities, see, e.g., [15].

Intrinsic to the BFM formalism is the duplication of the number of gauge fields, which are distinguished into “background” and “quantum” types [8, 10]; while the former are not integrated over in the path integral and do not appear in loops, the latter are identified with the standard gauge fields known from the conventional formulation, e.g., in the linear covariant gauges [18].

The correlation (Green’s) functions built out of background fields satisfy linear Slavnov-Taylor identities (STIs) [19, 20], which are naive generalizations of tree level relations, without deformations originating from the ghost-sector of the theory. In addition, and more importantly for our purposes, they are connected to the corresponding Green’s functions involving quantum fields by exact relations, known as “background-quantum identities” (BQIs) [15, 21–23]. These special identities are derived with the aid of the Batalin-Vilkovisky (BV) formalism [24, 25], where the original BFM action is extended

through the inclusion of suitable anti-fields and sources.

The common ingredient of this infinite tower of identities is a particular function, denoted by  $G(q)$ , which we denominate “BV function” [23]. The precise field-theoretic definition of this function involves a special combination of an anti-field and a source; however, a more practical relation expresses  $G(q)$  in terms of the conventional gluon and ghost propagators, and the ghost-gluon kernel, known from the STI satisfied by the three-gluon vertex [26–33].

The BV function appears in a variety of non-perturbative applications, such as the so-called “block-wise” truncations of the SDE series [34–38], and the definition of an effective interaction which is both RGI and process-independent [39, 40], constituting a common component of every two-to-two on-shell process. In addition,  $G(q)$  is related to the inverse of the ghost dressing function through an exact relation [40–43], which enforces the coincidence of distinct versions of effective charges in the deep infrared [40]. In that sense, the BV function represents an essential component of the gauge sector of Yang-Mills theories, participating non-trivially in the description of the associated dynamics.

Particularly pivotal to the present analysis is the *Landau-gauge* equality between the BV function and the so-called Kugo-Ojima (KO) function [41, 44], whose field-theoretic definition is especially suitable for a lattice simulation [45–48]. Exploiting this key relation, we carry out a large-volume simulation of the KO function, and thus, we simultaneously obtain the lattice result for the BV function.

The lattice results are contrasted with those obtained from the corresponding SDE that governs the evolution of  $G(q)$ , finding rather good agreement. In addition, the aforementioned rela-

tion between  $G(q)$  and the ghost dressing function is shown to be fulfilled at a reasonable level of accuracy. Furthermore, the lattice results for  $G$ , together with the data for the gluon propagator obtained from the same lattice, allow us to present the first purely lattice-based construction of the effective interaction introduced in [49, 50].

## 2. The ubiquitous Batalin-Vilkovisky function

Within the BFM approach, the gauge field  $A$  appearing in the classical action is decomposed as  $A = B + Q$ , where  $B$  and  $Q$  are the background and quantum (fluctuating) fields, respectively. Background fields participate in Feynman diagrams only as external legs, while loops are comprised exclusively by quantum fields [8, 10]. The key property of the BFM is that the gauge-fixing may be implemented without compromising explicit gauge invariance. Specifically, instead of the gauge-fixing term

$$\mathcal{L}_{\text{gf}} = \frac{1}{2\xi}(\partial_\mu Q^{a\mu})^2, \quad (1)$$

of the conventional covariant ( $R_\xi$ ) gauges [18], one uses

$$\widehat{\mathcal{L}}_{\text{gf}} = \frac{1}{2\xi_Q}(\widehat{D}_\mu^{ab} Q^{b\mu})^2, \quad \widehat{D}_\mu^{ab} = \partial_\mu \delta^{ab} + g f^{abc} B_\mu^c, \quad (2)$$

where  $f^{abc}$  are the structure constants of SU(3). The key feature that converts the BFM into a powerful quantization scheme is that the gauge-fixing choice of Eq. (2) gives rise to a gauge-fixed action which is invariant under gauge transformations of the background field,  $\delta B_\mu^a = -g^{-1} \partial_\mu \theta^a + f^{abc} \theta^b B_\mu^c$ , where  $g$  denotes the gauge coupling.

A profound consequence of this invariance is the form of the resulting STIs. Specifically, when Green's functions are contracted by the momentum carried by one of their background gluons, they satisfy *ghost-free* STIs, akin to the Takahashi identities [51, 52] known from Abelian theories, such as QED. These special STIs have far-reaching consequences for renormalization, because they impose QED-like constraints among the various renormalization constants. In particular, the wavefunction renormalization constant of the  $B$  field,  $Z_B$ , and the gauge coupling renormalization constant,  $Z_g$ , defined as

$$B_r^{a\mu} = Z_B^{-1/2} B^{a\mu}, \quad g_r = Z_g^{-1} g, \quad (3)$$

satisfy the key relation (see, *e.g.*, [8, 10])

$$Z_g = Z_B^{-1/2}, \quad (4)$$

in close analogy to the textbook relation  $Z_e = Z_A^{-1/2}$ , obeyed by the renormalization constants of the electric charge and the photon [53].

In what follows we will identify the quantum gauge-fixing parameter  $\xi_Q$  of the BFM [see Eq. (2)] with the corresponding parameter  $\xi$  of the covariant gauges [see Eq. (1)], *i.e.*,  $\xi_Q = \xi$ ; in particular, in the Landau gauge that we adopt throughout this work,  $\xi_Q = \xi = 0$ . With this identification, the propagator

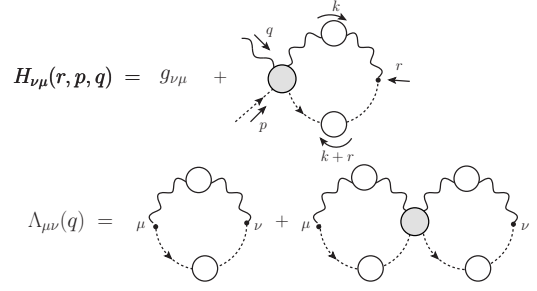


Figure 1: Diagrammatic definitions of the ghost-gluon scattering kernel,  $H_{\nu\mu}(r, p, q)$ , and the two-point function  $\Lambda_{\mu\nu}(q)$ , given in Eq. (8).

$\Delta_{\mu\nu}^{ab}(q) = -i\delta^{ab} \Delta_{\mu\nu}(q)$  that connects two quantum gluons coincides with the standard gluon propagator of the  $R_\xi$  gauges; in the Landau gauge,  $\Delta_{\mu\nu}(q)$  is completely transverse, *i.e.*,

$$\Delta_{\mu\nu}(q) = \Delta(q) P_{\mu\nu}(q), \quad P_{\mu\nu}(q) := g_{\mu\nu} - q_\mu q_\nu / q^2. \quad (5)$$

In addition to  $\Delta_{\mu\nu}^{ab}(q)$ , in the BFM we have two more gluon propagators, one connecting the fields  $Q_\mu^a(q)$  with a  $B_\nu^b(-q)$ , and one connecting  $B_\mu^a(q)$  with a  $B_\nu^b(-q)$ ; the latter is essential for the ensuing analysis, and will be denoted by

$$\widehat{\Delta}_{\mu\nu}^{ab}(q) = -i\delta^{ab} \widehat{\Delta}(q) P_{\mu\nu}(q). \quad (6)$$

It turns out that the gluon propagators  $\Delta(q)$  and  $\widehat{\Delta}(q)$  are related by the simplest of all BQIs, namely [21, 23, 42, 54]

$$\Delta(q) = [1 + G(q)]^2 \widehat{\Delta}(q). \quad (7)$$

$G(q)$  is the  $g_{\mu\nu}$  component of a certain two-point function,  $\Lambda_{\mu\nu}(q)$ , given by (Minkowski space)

$$\begin{aligned} \Lambda_{\mu\nu}(q) &:= ig^2 C_A \int_k \Delta_\mu^a(k) D(k+q) H_{\nu\rho}(-q, k+q, -k) \\ &= \underbrace{G(q)}_{\text{BV function}} g_{\mu\nu} + L(q) \frac{q_\mu q_\nu}{q^2}, \end{aligned} \quad (8)$$

where  $C_A$  is the Casimir eigenvalue of the adjoint representation [ $N$  for SU( $N$ )],  $D^{ab}(q) = i\delta^{ab} D(q)$  is the ghost propagator, and  $H_{\nu\mu}(r, p, q)$  denotes the ghost-gluon kernel, see upper panel of Fig. 1. Note that, formally,  $\Lambda_{\mu\nu}(q)$  is a two-point function of a background source,  $\Omega_\mu^a$ , and a gluon anti-field,  $A_\nu^{b*}$ , usually denoted in the literature by  $\Gamma_{\Omega_\mu^a A_\nu^{b*}}(q)$ ; the version given in Eq. (8) [see lower panel of Fig. 1] relies on the fact that  $\Omega_\mu^a$  and  $A_\nu^{b*}$  may be replaced by the Becchi-Rouet-Stora-Tyutin (BRST) [55, 56] composite operator to which they are coupled.

Next, consider three-point functions (vertices) of the general type  $\Gamma_{BXY}$  and  $\Gamma_{AXY}$  where  $X$  and  $Y$  represent general fields (*e.g.*,  $X = Y = A$  in the case of a three-gluon vertex, or  $X = \psi$ ,  $Y = \bar{\psi}$  for the quark-gluon vertex). The vertex BQI has the general form

$$\Gamma_{BXY} = [1 + G(q)] \Gamma_{AXY} + \dots, \quad (9)$$

where the ellipsis denotes terms that involve additional auxiliary functions, and vanish "on shell".

Higher correlation functions are related by similar, albeit increasingly more complicated BQIs, with the BV function playing always a prominent role [36].

We next turn to a special identity that relates the two form factors  $G(q)$  and  $L(q)$  of  $\Lambda_{\mu\nu}(q)$  with the ghost dressing function,  $F(q)$ , defined as

$$F(q) = q^2 D(q). \quad (10)$$

Specifically, in the Landau gauge, we have the exact relation [40, 49, 54]

$$F^{-1}(q) = 1 + G(q) + L(q). \quad (11)$$

Due to the fact that the function  $L(q)$  vanishes at the origin,  $L(0) = 0$  [40], from Eq. (11) we obtain the important result

$$F^{-1}(0) = 1 + G(0). \quad (12)$$

Note that this last relation enforces the coincidence between the Taylor [12, 57–67] and "pinch-technique" [15, 39, 68] effective charges in the deep infrared [69, 70]

### 3. Schwinger-Dyson equations for $G(q)$ and $L(q)$

Within the standard framework of the SDEs, the dynamical equations that govern the momentum evolution of  $G(q)$  and  $L(q)$  may be deduced directly from Eq. (8) by projecting out the  $g_{\mu\nu}$  and  $q_\mu q_\nu / q^2$  components, respectively [40]; the tensorial decomposition [32]

$$H_{\nu\mu}(r, p, q) = g_{\nu\mu} A_1 + r_\mu r_\nu A_2 + q_\mu q_\nu A_3 + r_\mu q_\nu A_4 + r_\nu q_\mu A_5, \quad (13)$$

with  $A_i := A_i(r, p, q)$ , is also employed.

Setting  $f := 1 - (q \cdot k)^2 / (q^2 k^2)$  and  $\tilde{A}_i := A_i(-q, k + q, -k)$ , we obtain

$$\begin{aligned} 1 + G(q) &= Z_c + \frac{ig^2 C_A}{3} \int_k \Delta(k) D(k+q) K_G, \\ L(q) &= \frac{ig^2 C_A}{3} \int_k \Delta(k) D(k+q) K_L, \end{aligned} \quad (14)$$

where

$$\begin{aligned} K_G &= (3-f)\tilde{A}_1 - (k \cdot q) f \tilde{A}_4, \\ K_L &= (3-4f)\tilde{A}_1 - f [3q^2 \tilde{A}_2 + 4(q \cdot k) \tilde{A}_4], \end{aligned} \quad (15)$$

and

$$\int_k := \frac{1}{(2\pi)^4} \int_{-\infty}^{+\infty} d^4 k \quad (16)$$

is the properly regularized measure.

Note that, due to the validity of Eq. (11), the  $G(q)$  in Eq. (14) is renormalized through the  $Z_c$ , namely the ghost renormalization constant. For its determination, one must consider the corresponding SDE for the ghost dressing function  $F(q)$ , see, e.g., [38]. This dynamical equation involves the ghost-gluon vertex as one of its ingredients; this latter vertex is finite in the Landau gauge, and its attendant renormalization constant,  $Z_1$ , is independent of the cutoff. Within the Taylor

scheme [62, 71, 72] that we will employ, we have  $Z_1 = 1$ , and the SDE for  $F(q)$  assumes the form

$$F^{-1}(q) = Z_c + ig^2 C_A \int_k f \Delta(k) D(k+q) \tilde{B}_1, \quad (17)$$

where  $\tilde{B}_1 := B_1(-q, k + q, -k)$ , with  $B_1$  denoting the classical form factor of the ghost-gluon vertex. Then, the expression for  $Z_c$  to be used in Eq. (14) is obtained from Eq. (17) by imposing the renormalization condition  $F(\mu) = 1$ , where  $\mu$  is the renormalization point; throughout this work we use  $\mu = 4.3$  GeV.

The numerical treatment of the SDE system formed by Eqs. (14) and (17) proceeds along the lines described in [40, 73], using up-to-date ingredients as external inputs. Specifically, we employ general kinematics results for  $\tilde{B}_1$  and  $\tilde{A}_i$ , determined from their own SDEs in [32]; instead, in [40, 73] these form factors were set at their tree-level values. Moreover, we employ directly a fit to the lattice gluon propagator  $\Delta(q)$  (lower panel of Fig. 4), obtained from the same lattice setups used for the determination of  $1 + G(q)$  and  $F(q)$ . The resulting SDE solutions for  $G(q)$  and  $L(q)$  will be discussed in Sec. 5.

### 4. Lattice simulation: theory and setup

Both the formal definition of  $G(q)$  in terms of BV fields and the alternative presented in Eq. (8) are unsuitable for performing lattice simulations. Instead, we will take advantage of the known equality between  $G(q)$  and the KO function<sup>1</sup>, to be denoted by  $u(q)$ ; specifically, in the Landau gauge, we have [41–43, 73].

$$G(q) = u(q). \quad (18)$$

The field-theoretic definition of  $u(q)$  that has been implemented on the lattice involves two composite operators,

$$\mathcal{A}_\mu^a(x) := D_\mu^{ae}(x) c^e(x), \quad \mathcal{B}_\nu^b(x) := f^{bcd} A_\nu^d(x) \bar{c}^c(x), \quad (19)$$

where  $D_\mu^{ab}(x) = \partial_\mu \delta^{ac} + g f^{abc} A_\mu^c(x)$  is the covariant derivative in the adjoint representation, and the two-point function  $\mathcal{U}_{\mu\nu}^{ab}(q)$ , defined as (Euclidean space)

$$\mathcal{U}_{\mu\nu}^{ab}(q) = \int d^4 x e^{iq(x-y)} \langle 0 | T (\mathcal{A}_\mu^a(x) \mathcal{B}_\nu^b(y)) | 0 \rangle, \quad (20)$$

where  $T$  denotes the standard time-ordering operation. The KO function is the scalar co-factor of  $\mathcal{U}_{\mu\nu}^{ab}(q)$ ,

$$\mathcal{U}_{\mu\nu}^{ab}(q) = \delta^{ab} \left( \delta^{\mu\nu} - \frac{q_\mu q_\nu}{q^2} \right) u(q). \quad (21)$$

An explicit lattice definition for  $\mathcal{U}_{\mu\nu}^{ab}(q)$  is given by

$$\mathcal{U}_{\mu\nu}^{ab}(q) = \frac{1}{V} \left\langle \sum_{x,y,z,c,d,e} e^{-iq \cdot (x-y)} (D_\mu)^{ae}(x; z) (M^{-1})^{ec}(z; y) f^{bcd} A_\nu^d(y) \right\rangle_U \quad (22)$$

<sup>1</sup>This function is associated with a standard confinement criterion [41, 44]; for a review, see [12]. It is well-known that the  $u$  simulated on the lattice does not comply with this criterion [45, 46], nor do the "decoupling" propagators, see, e.g., [74–77] and [37, 78, 79].

where  $\langle \dots \rangle_U$  denotes the Monte-Carlo sample average over the gauge field configurations  $U$ , and  $M$  is a suitably discretized version of the Faddeev-Popov operator,  $\partial_\mu D_\mu^{ab}$ ; note that the inverse of  $M$  is related to the ghost propagator by

$$D^{ab}(q) = \int d^4x e^{iq(x-y)} \langle 0|T(M^{-1})^{ab}(x;y)|0\rangle. \quad (23)$$

With the aid of Eq. (21), the scalar function  $u(q)$  is given by

$$u(q) = \frac{1}{24} \sum_{\mu,a} \mathcal{U}_{\mu\mu}^{aa}(q). \quad (24)$$

In order to study the KO function on the lattice, we rely on Eq. (22). However, for practical reasons, it is convenient to compute  $\mathcal{U}_{\mu\nu}^{ab}(q)$  using a point source  $y_0$  in the inversion of the lattice Faddeev-Popov operator,  $M$ ,

$$\mathcal{U}_{\mu\nu}^{ab}(q) = \left\langle \sum_{x,z} \sum_{c,d,e} e^{-iq(x-y_0)} (D_\mu)^{ae}(x;z) (M^{-1})^{ec}(z;y_0) f^{bcd} A_\nu^d(y_0) \right\rangle_U \quad (25)$$

where the lattice definitions for  $D$ ,  $M$ , and  $A$  can be found in [46, 80, 81].

The most important points of the lattice simulation may be summarized as follows:

(i) The gauge field,  $A_\mu^a$ , covariant derivative,  $D_\mu^{ab}$ , and Faddeev-Popov operator,  $M_{xy}^{ab}$ , are suitably discretized according to [46, 47, 77, 82].

(ii) The Landau gauge is fixed by identifying the configurations belonging to the Gribov region; this is achieved through the maximization of a certain functional, whose discretized form is given in [46, 47]. Numerically, the required maximization is performed with the Fourier Accelerated Steepest Descent method [83].

(iii) Since  $M_{xy}^{ab}$  is a singular operator, it can only be inverted in the subspace orthogonal to its zero modes. Nevertheless, this is sufficient for computing  $u(q)$  for  $q \neq 0$  [81]. In this case, the inversion problem in the orthogonal subspace can be transformed into a sparse linear system of equations, as explained in detail in [46, 47, 81]. Then, since  $M_{xy}^{ab}$  is real and symmetric, the resulting system can be solved efficiently with the conjugate gradient method [84].

(iv) We consider quenched lattice ensembles generated with the Wilson gauge action [85], with  $\beta = 6.0$ . In this case, the Sommer parameter method [86] yields a lattice spacing of  $a = 0.0962$  fm ( $a^{-1} = 2.05$  GeV) [87]. We employ two setups, with lattice volumes  $V = 64^4$ , and  $V = 80^4$ , in lattice units; the corresponding physical volumes extend from  $(6 \text{ fm})^4$  to  $(8 \text{ fm})^4$ . Further details on sampling, gauge fixing, and definitions can be found in [88].

(v) The number of gauge field configurations considered for the present study was 700 for  $V = 64^4$ , and 500 for  $V = 80^4$ .

(vi) The computer simulations were performed with the help of the Chroma library [89], using PFFT [90] for the necessary Fourier transforms.

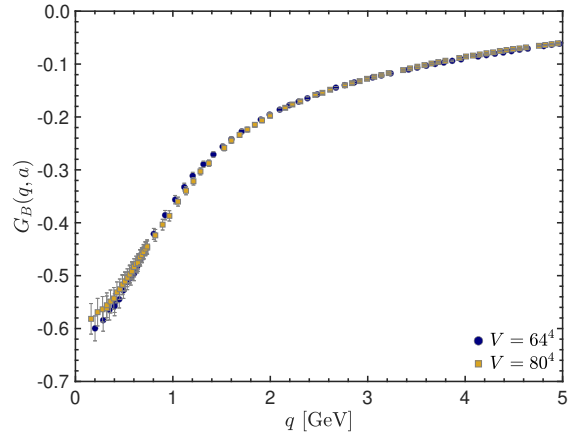


Figure 2: Bare lattice results for the BV function,  $G_B(q, a)$ .

## 5. Results

Even though the lattice simulation uses the expression in Eq. (21) as its starting point, in what follows we present the results in terms of  $G(q)$ , which is the focal point of this study, rather than  $u(q)$ . Evidently, by virtue of Eq. (18), the results may be recast trivially in terms of  $u(q)$ , by setting  $G \rightarrow u$  throughout.

Let us denote the bare  $G(q)$  obtained on the lattice by  $G_B(q, a)$ , making manifest the dependence on the lattice spacing  $a$ . The result for  $G_B(q, a)$  from our simulations are shown in Fig. 2, for both lattice volumes. We note that the volume dependence is rather weak; indeed, the data from both volumes agree within errors.

Ideally, in order to obtain a reliable comparison with the SDE results, the  $G_B(q, a)$  should be extrapolated to the continuum limit,  $a \rightarrow 0$ , and be renormalized using the Taylor scheme. Instead, in what follows we adopt a slightly modified version of the procedure developed in [46], whereby  $G_B(q, a)$  is renormalized by imposing Eq. (11).

To begin with, the continuum limit  $G_B(q) := G_B(q, 0)$  is related to the lattice  $G_B(q, a)$  by

$$G_B(q, a) = G_B(q) + s(q), \quad (26)$$

where  $s(q)$  accounts for lattice artifacts, and, in principle, depends on the momentum  $q$ . However, the momentum dependence of  $s(q)$  cannot be determined by the analysis employed below. Therefore, in order to proceed, we *assume* that the dependence of  $s(q)$  on the momentum is fairly mild [77] and treat it as a constant, *i.e.*,  $s(q) \rightarrow s$ .

Then, the renormalized lattice  $1 + G(q)$  in the Taylor scheme is given by

$$1 + G(q) = Z_c[1 + G_B(q, a) - s], \quad (27)$$

where the parameter  $s$  acts as an effective subtractive renormalization constant. We emphasize that subtractive terms in the renormalization have been shown to improve the agreement with the continuum theory in studies of the quark propagator and the quark-gluon vertex [91, 92].

The value of  $Z_c$  can be determined formally by imposing a renormalization condition, *i.e.*, a value for the renormalized  $1 + G(\mu)$ , at some scale  $\mu$ . However, since in the Taylor scheme  $F(\mu) = 1$ , and  $L(\mu)$  generally does not vanish, Eq. (11) implies that we cannot impose  $1 + G(\mu) = 1$ .

Instead, we determine the value of  $1 + G(\mu)$  by first computing  $1 + G(q)$  at one loop,

$$1 + G^{(1)}(q) = 1 + \frac{\alpha_s C_A}{16\pi} [3 \ln(q^2/\mu^2) - 2], \quad (28)$$

with  $\alpha_s = g^2/4\pi$ . Then, using the value of  $\alpha_s = 0.216$  for the Taylor coupling at  $\mu = 4.3$  GeV [62] we obtain

$$1 + G^{(1)}(\mu) = 0.974. \quad (29)$$

Interestingly, the SDE result yields  $1 + G(\mu) = 0.973$ , indicating that the perturbative regime of  $1 + G(q)$  has been safely reached for  $q = \mu = 4.3$  GeV. Hence, we can fix the scale of the lattice  $1 + G(q)$  by imposing  $1 + G(\mu) = 1 + G^{(1)}(\mu)$ , such that

$$Z_c = \frac{1 + G^{(1)}(\mu)}{1 + G_B(\mu, a) - s} = \frac{0.974}{0.922 - s}, \quad (30)$$

where used  $G_B(\mu, a) = -0.078$ , obtained from the bare data of Fig. 2.

At this point,  $Z_c$  still depends on the unknown constant  $s$ . To fix its value, we impose the validity of Eq. (11), *i.e.*,

$$Z_c [1 + G_B(q, a) - s] + L(q) = F_{\text{lat}}^{-1}(q), \quad (31)$$

where  $F_{\text{lat}}(q)$  is the renormalized lattice ghost dressing function, obtained self-consistently from the same lattice setups used to compute  $G_B(q, a)$ .

Now, the function  $L(q)$  is not directly computed on the lattice. Nevertheless, for small  $q$  we can assume for  $L(q)$  a Taylor expansion,

$$L(q) = a_1 q^2 + a_2 q^4 + O(q^6), \quad (32)$$

whose 0-th order term vanishes on account of  $L(0) = 0$ .

Then, we can determine the parameters  $s$ ,  $a_1$ , and  $a_2$ , by rephrasing Eq. (31) as a  $\chi^2$  minimization problem. Specifically, we minimize the  $\chi^2$  defined by

$$\chi^2 := \sum_i \{Z_c [1 + G_B(q_i, a) - s] + a_1 q_i^2 + a_2 q_i^4 - F_{\text{lat}}^{-1}(q_i)\}^2, \quad (33)$$

where  $q_i$  are the lattice points, and  $Z_c$  is given by Eq. (30).

Since Eq. (33) is the result of a Taylor expansion, it is supposed to be used only for small  $q$ ; specifically, we choose the points  $q_i < 0.5$  GeV. Consequently, there are too few points to reliably determine the parameters  $s$ ,  $a_1$  and  $a_2$  for the two lattice setups individually. Instead, we apply the above procedure to the *combined* data points of both volumes, for which there are 18 points in the fitting window. We have verified that for the combined data, the value of  $s$  is stable against varying the order of the Taylor expansion in Eq. (32), as well as the fitting window. Specifically, we obtain  $s = 0.121$ ,  $a_1 = 0.458$  GeV<sup>-2</sup>, and  $a_2 = -0.905$  GeV<sup>-4</sup>, for which  $\chi^2 = 2 \times 10^{-3}$ .

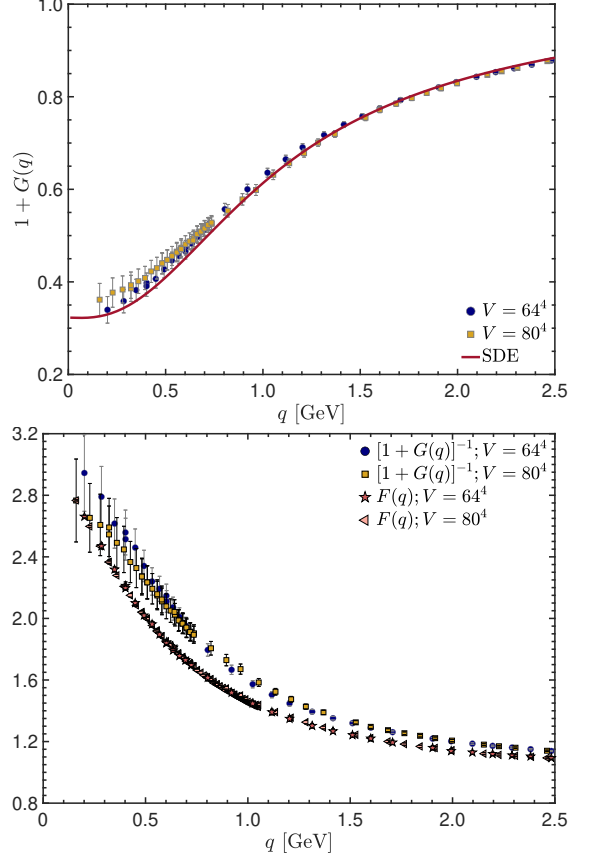


Figure 3: Top: Results for  $1 + G(q)$  obtained from the lattice (points) and the SDE prediction (red curve). Bottom: Comparison of  $[1 + G(q)]^{-1}$  (circles/squares) and  $F(q)$  (stars/triangles).

Using the above value of  $s$  in Eqs. (27) and (30), we obtain the renormalized lattice  $1 + G(q)$ , shown as points on the top panel of Fig. 3. On the same panel we show also the SDE prediction (red continuous), finding an excellent agreement. On the bottom panel of Fig. 3, we compare  $F(q)$  to  $[1 + G(q)]^{-1}$ ; evidently, Eq. (12) is satisfied within errors, as a consequence of the renormalization procedure employed.

The comparison between lattice and SDE results may be taken a step further, by considering the full momentum dependence of the form factor  $L(q)$ . In particular, a lattice-derived result for  $L(q)$  may be obtained from Eq. (11), by substituting in it the lattice data for  $F(q)$  and  $1 + G(q)$ . The outcome of this procedure is shown in Fig. 4; the comparison with the SDE prediction (red continuous curve) reveals a reasonable agreement. The blue curve represents a fit to the lattice  $L(q)$ , given by the simple functional form

$$L(q) = \frac{q^2/c_1^2 + (q^2/c_2^2)^2}{1 + q^2/t_1^2 + (q^2/t_2^2)^2 \ln^{d_L}(1 + q^2/\Lambda_T^2)}, \quad (34)$$

where  $\Lambda_T = 425$  MeV is the value of  $\Lambda_{\text{QCD}}$  in the Taylor scheme [62], and  $d_L = 35/44$  is the anomalous dimension of  $L(q)$  [93]. The fitting parameters are given by  $c_1^2 = 2.18$  GeV<sup>2</sup>,  $c_2^2 = 0.575$  GeV<sup>2</sup>,  $t_1^2 = 0.0981$  GeV<sup>2</sup>, and  $t_2^2 = 0.188$  GeV<sup>2</sup>. Note that Eq. (34) satisfies  $L(0) = 0$  by construction.

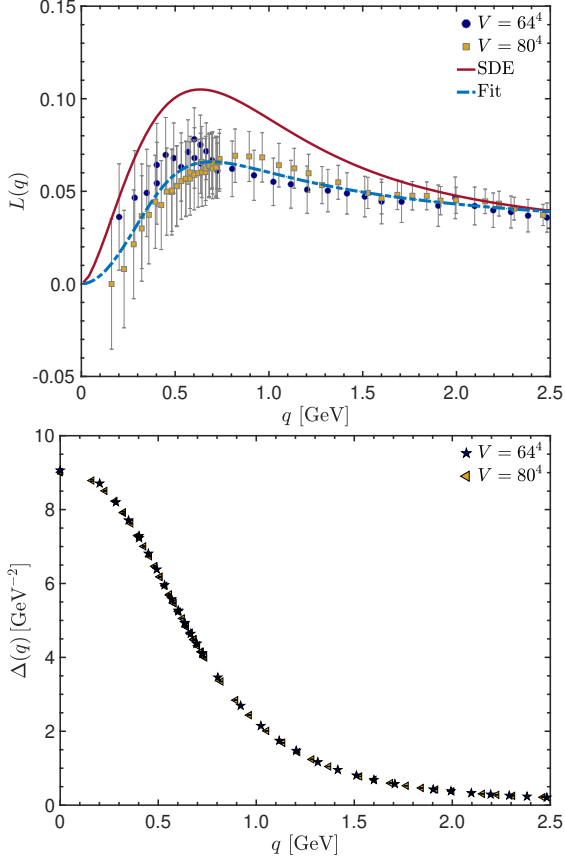


Figure 4: Upper panel:  $L(q)$  obtained from the lattice  $1 + G(q)$  and  $F(q)$  of Fig. 3 (points) compared to the SDE prediction (red continuous). Also shown is a fit given by Eq. (34) (blue dashed). Lower panel: The gluon propagator simulated on the same lattices as the BV function [94].

## 6. RGI running interaction strength

As has been explained in a series of articles [15, 40, 49], the fundamental relation of Eq. (4) allows for the definition of a propagator-like RGI quantity, exactly as happens in QED when the photon vacuum polarization is multiplied by  $e^2$ . In particular, since  $\widehat{\Delta}(q)$  renormalizes through the  $Z_B$  introduced in Eq. (4), *i.e.*,

$$\widehat{\Delta}_R(q) = Z_B^{-1} \widehat{\Delta}(q), \quad (35)$$

the combination

$$\widehat{d}(q) := \alpha_s \widehat{\Delta}(q), \quad (36)$$

is RGI by virtue of Eq. (4). Indeed,  $\widehat{d}(q)$  retains exactly the same form before and after renormalization, and, consequently, does not depend on the renormalization point  $\mu$ , nor on the renormalization scheme employed.

The BV function enters into the definition of  $\widehat{d}(q)$  when the central relation in Eq. (7) is invoked,

$$\widehat{d}(q) := \frac{\alpha_s \Delta(q)}{[1 + G(q)]^2}; \quad (37)$$

in this form,  $\widehat{d}(q)$  is known in the literature as the ‘‘RGI running interaction strength’’ [49].

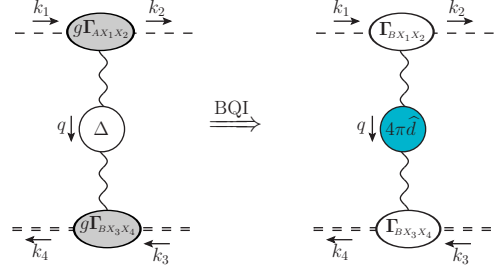


Figure 5: Diagrammatic representation of the BQI-induced rearrangement in the case of a generic  $X_1 X_2 \rightarrow X_3 X_4$  scattering, corresponding to the S-matrix element  $\mathcal{T}_{X_1 X_2 \rightarrow X_3 X_4}$  of Eq. (38).

What is particularly interesting about  $\widehat{d}(q)$  is that it does not represent a mere field-theoretic construct, but admits a clear physical interpretation. Specifically,  $\widehat{d}(q)$  constitutes a common component of any two-to-two physical processes,  $X_1(k_1) X_2(k_2) \rightarrow X_3(k_3) X_4(k_4)$ , where an off-shell gluon, carrying momentum  $q = k_1 - k_2 = k_3 - k_4$ , is exchanged, see Fig. 5. In particular, with the aid of the BQIs in Eqs. (7) and (9), the S-matrix element  $\mathcal{T}_{X_1 X_2 \rightarrow X_3 X_4}$  may be cast in the form

$$\begin{aligned} \mathcal{T}_{X_1 X_2 \rightarrow X_3 X_4} &= \{g \Gamma_{AX_1 X_2}\} \Delta(q) \{g \Gamma_{AX_3 X_4}\} \\ &= \{g [1 + G(q)]^{-1} \Gamma_{BX_1 X_2}\} \Delta(q) \{g [1 + G(q)]^{-1} \Gamma_{BX_3 X_4}\} \\ &= \Gamma_{BX_1 X_2} \underbrace{\{g^2 [1 + G(q)]^{-2} \Delta(q)\}}_{4\pi \widehat{d}(q)} \Gamma_{BX_3 X_4}. \end{aligned} \quad (38)$$

Due to the general validity of the BQIs, the steps leading to the last line of Eq. (38) may be followed regardless of the detailed nature of the initial and final states. In that sense,  $\widehat{d}(q)$  captures the process-independent contribution, common to all such processes, whilst the process-dependence, *i.e.*, the part that carries the information about the specific nature of the initial and final states, is encoded in the vertices  $\Gamma_{BX_1 X_2}$  and  $\Gamma_{BX_3 X_4}$ .

The quantity  $\widehat{d}(q)$  has mass dimension of  $-2$ ; from it one may define the dimensionless RGI interaction  $\mathcal{I}(q)$  [49]

$$\mathcal{I}(q) := q^2 \widehat{d}(q). \quad (39)$$

As explained in [49], this quantity provides the strength required in order to describe ground-state hadron observables using SDEs in the matter sector of the theory. As was argued there, the physics encoded in  $\mathcal{I}(q^2)$  reconciles nonperturbative continuum QCD with *ab initio* predictions of basic hadron properties.

In Fig. 6, the red continuous curves correspond to the  $\widehat{d}(q)$  (top) and  $\mathcal{I}(q)$  (bottom), obtained by combining the  $1 + G(q)$  from Fig. 3 with the gluon propagator, self-consistently simulated on the same lattice setups (see lower panel of Fig. 4). For the Taylor coupling at  $\mu = 4.3$  GeV, we use  $\alpha_s = 0.216$  [62]; note that, due to the RGI nature of  $\widehat{d}(q)$ , any other set  $\{\mu, \alpha_s(\mu)\}$  yields precisely the same answer. In addition, the  $\widehat{d}(q)$  and  $\mathcal{I}(q)$  obtained from the SDE analysis of [49] are displayed as green dotted curves. Note that the present treatment leads to closer agreement between lattice and SDE results; we have confirmed

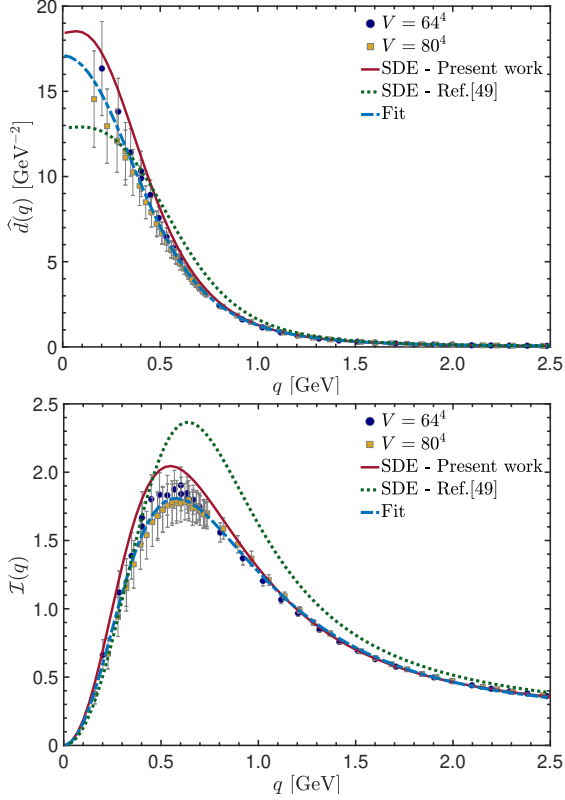


Figure 6: Lattice results for  $\widehat{d}(q)$  (top) and  $\mathcal{I}(q)$  (bottom), represented by points. On both panels, the present SDE result (red continuous curve) and that of [49] (green dotted) are shown for comparison. The fit to the lattice data, given by Eq. (40) is shown in blue dashed.

that this is mainly due to the non-perturbative dressing of the form factors  $\widetilde{B}_1$  and  $\widetilde{A}_7$ , discussed in the last paragraph of Sec. 3.

Moreover, in Fig. 6 we show as a blue dashed curve a fit to the lattice  $\widehat{d}(q)$ , given by the functional form

$$\widehat{d}(q) = \frac{\widehat{d}(0) [1 + a_1 q^2 + a_2 q^4]}{1 + b_1 q^2 + b_2 q^4 + \beta_0 \widehat{d}(0) a_2 q^6 \ln(1 + q^2/\Lambda_\tau^2)}, \quad (40)$$

where  $\beta_0 = 11/(4\pi)$  is the first coefficient of the QCD beta function,  $\Lambda_\tau = 425$  MeV [62], and the fitting parameters are  $\widehat{d}(0) = 17.1$  GeV $^{-2}$ ,  $a_1 = 0.0585$  GeV $^{-2}$ ,  $a_2 = 0.0274$  GeV $^{-4}$ ,  $b_1 = 3.51$  GeV $^{-2}$ ,  $b_2 = 9.33$  GeV $^{-4}$ . Note that Eq. (40) enforces the one loop-running of the QCD coupling in the ultraviolet, *i.e.*,  $\mathcal{I}(q) \rightarrow [\beta_0 \ln(q^2/\Lambda_\tau^2)]^{-1}$  at large  $q$ .

## 7. Conclusions

The quantitative agreement between the BV function simulated on the lattice and the corresponding SDE results exposes once again the underlying consistency of a large number of concepts and techniques, developed over a period of several years, see, *e.g.*, [95]. Especially interesting in that regard is the interplay between the ghost and gauge sectors of the theory, which are nontrivially intertwined by the SDEs. Note, in particular, that the lattice gluon propagator in Fig. 4 is used as input in the SDEs of Eqs. (14) and (17), which produce the prediction for

$G(q)$  that is subsequently compared with the corresponding lattice result in Fig. 3. Let us finally emphasize that the effective interactions  $\widehat{d}(q)$  and  $\mathcal{I}(q)$  shown in Fig. 6 correspond to the pure Yang-Mills case; for phenomenological applications they must be modified to include effects from dynamical quarks, in the spirit of [50, 93, 96]. In fact, the results of the present work bolster up our confidence in the SDE derivations that lead to the "unquenching" of these RGI quantities.

## Acknowledgements

The authors acknowledge the computing time provided by the Laboratory for Advanced Computing at the University of Coimbra (FCT contracts 2021.09759.CPCA and 2022.15892.CPCA.A2). Work supported by FCT contracts CERN/FIS-PAR/0023/2021, UIDB/04564/2020, and UIDP/04564/2020. P. J. S. acknowledges financial support from FCT under Contract No. CEECIND/00488/2017. A. C. A is supported by the CNPq grant 310763/2023-1, and acknowledges financial support from project 464898/2014-5 (INCT-FNA). M. N. F. and J. P. are supported by the Spanish MICINN grant PID2020-113334GB-I00. M. N. F. acknowledges financial support from Generalitat Valenciana through contract CIAPOS/2021/74. J. P. also acknowledges funding from the Generalitat Valenciana grant CIPROM/2022/66. This work was granted access to the HPC resources of the PDC Center for High Performance Computing at the KTH Royal Institute of Technology, Sweden, made available within the Distributed European Computing Initiative by the PRACE-2IP, receiving funding from the European Community's Seventh Framework Programme (FP7/ 2007-2013) under grant agreement No. RI-283493. The use of Lindgren has been provided under DECI-9 project COIMBRALATT. We acknowledge that the results of this research have been achieved using the PRACE-3IP project (FP7 RI- 312763) resource Sisu based in Finland at CSC. The use of Sisu has been provided under DECI-12 project COIMBRALATT2.

## References

- [1] B. S. DeWitt, Phys. Rev. 162 (1967) 1195–1239.
- [2] J. Honerkamp, Nucl. Phys. B 48 (1972) 269–287.
- [3] R. E. Kallosh, Nucl. Phys. B 78 (1974) 293–312.
- [4] H. Kluberg-Stern, J. B. Zuber, Phys. Rev. D 12 (1975) 482–488.
- [5] I. Y. Arefeva, L. D. Faddeev, A. A. Slavnov, Theor. Math. Phys. 21 (1975) 1165.
- [6] L. Abbott, Nucl. Phys. B 185 (1981) 189–203.
- [7] S. Weinberg, Phys. Lett. B91 (1980) 51.
- [8] L. F. Abbott, Acta Phys. Polon. B13 (1982) 33.
- [9] G. M. Shore, Annals Phys. 137 (1981) 262.
- [10] L. F. Abbott, M. T. Grisaru, R. K. Schaefer, Nucl. Phys. B 229 (1983) 372–380.
- [11] C. D. Roberts, A. G. Williams, Prog. Part. Nucl. Phys. 33 (1994) 477–575.
- [12] R. Alkofer, L. von Smekal, Phys. Rept. 353 (2001) 281.
- [13] C. S. Fischer, J. Phys. G 32 (2006) R253–R291.
- [14] C. D. Roberts, Prog. Part. Nucl. Phys. 61 (2008) 50–65.
- [15] D. Binosi, J. Papavassiliou, Phys. Rept. 479 (2009) 1–152.
- [16] I. C. Cloet, C. D. Roberts, Prog. Part. Nucl. Phys. 77 (2014) 1–69.
- [17] M. Q. Huber, Phys. Rept. 879 (2020) 1–92.
- [18] K. Fujikawa, B. W. Lee, A. I. Sanda, Phys. Rev. D6 (1972) 2923–2943.
- [19] J. Taylor, Nucl. Phys. B 33 (1971) 436–444.

- [20] A. Slavnov, *Theor. Math. Phys.* 10 (1972) 99–107.
- [21] P. A. Grassi, T. Hurth, M. Steinhauser, *Annals Phys.* 288 (2001) 197–248.
- [22] P. A. Grassi, T. Hurth, M. Steinhauser, *Nucl. Phys. B* 610 (2001) 215–250.
- [23] D. Binosi, J. Papavassiliou, *Phys. Rev. D* 66 (2002) 025024.
- [24] I. A. Batalin, G. A. Vilkovisky, *Phys. Lett. B* 69 (1977) 309–312.
- [25] I. A. Batalin, G. A. Vilkovisky, *Phys. Rev. D* 28 (1983) 2567–2582. [Erratum: *Phys. Rev. D* 30, 508 (1984)].
- [26] W. J. Marciano, H. Pagels, *Phys. Rept.* 36 (1978) 137.
- [27] J. S. Ball, T.-W. Chiu, *Phys. Rev. D* 22 (1980) 2550. [Erratum: *Phys. Rev. D* 23, 3085 (1981)].
- [28] P. Pascual, R. Tarrach, *Lect. Notes Phys.* 194 (1984) 1–277.
- [29] A. I. Davydchev, P. Osland, O. Tarasov, *Phys. Rev. D* 54 (1996) 4087–4113. [Erratum: *Phys. Rev. D* 59, 109901 (1999)].
- [30] J. A. Gracey, *Phys. Rev. D* 84 (2011) 085011.
- [31] J. Gracey, *Phys. Rev. D* 90 (2014) 025014.
- [32] A. C. Aguilar, M. N. Ferreira, C. T. Figueiredo, J. Papavassiliou, *Phys. Rev. D* 99 (2019) 034026.
- [33] A. C. Aguilar, M. N. Ferreira, C. T. Figueiredo, J. Papavassiliou, *Phys. Rev. D* 99 (2019) 094010.
- [34] A. C. Aguilar, J. Papavassiliou, *J. High Energy Phys.* 12 (2006) 012.
- [35] D. Binosi, J. Papavassiliou, *Phys. Rev. D* 77 (2008) 061702.
- [36] D. Binosi, J. Papavassiliou, *J. High Energy Phys.* 11 (2008) 063.
- [37] A. C. Aguilar, D. Binosi, J. Papavassiliou, *Phys. Rev. D* 78 (2008) 025010.
- [38] A. C. Aguilar, M. N. Ferreira, D. Ibañez, B. M. Oliveira, J. Papavassiliou, *Eur. Phys. J. C* 83 (2023) 86.
- [39] D. Binosi, J. Papavassiliou, *Nucl. Phys. Proc. Suppl.* 121 (2003) 281–284.
- [40] A. C. Aguilar, D. Binosi, J. Papavassiliou, J. Rodríguez-Quintero, *Phys. Rev. D* 80 (2009) 085018.
- [41] T. Kugo, in: *International Symposium on BRS Symmetry on the Occasion of Its 20th Anniversary*, arXiv:hep-th/9511033.
- [42] P. A. Grassi, T. Hurth, A. Quadri, *Phys. Rev. D* 70 (2004) 105014.
- [43] K.-I. Kondo, *Phys. Lett. B* 678 (2009) 322–330.
- [44] T. Kugo, I. Ojima, *Prog. Theor. Phys. Suppl.* 66 (1979) 1–130.
- [45] H. Nakajima, S. Furui, *Nucl. Phys. B Proc. Suppl.* 83 (2000) 521–523.
- [46] A. Sternbeck, *The Infrared behavior of lattice QCD Green’s functions*, Ph.D. thesis, Humboldt-University Berlin, arXiv:0609016.
- [47] N. M. R. Brito, *Lattice computation of the Kugo-Ojima correlation function*, Master thesis, University of Coimbra, arXiv:2310.09010.
- [48] N. Brito, O. Oliveira, P. J. Silva, J. Papavassiliou, M. N. Ferreira, A. C. Aguilar, *PoS LATTICE2023* (2024) 380.
- [49] D. Binosi, L. Chang, J. Papavassiliou, C. D. Roberts, *Phys. Lett. B* 742 (2015) 183–188.
- [50] Z.-F. Cui, J.-L. Zhang, D. Binosi, F. de Soto, C. Mezrag, J. Papavassiliou, C. D. Roberts, J. Rodríguez-Quintero, J. Segovia, S. Zafeiropoulos, *Chin. Phys. C* 44 (2020) 083102.
- [51] J. C. Ward, *Phys. Rev.* 78 (1950) 182.
- [52] Y. Takahashi, *Nuovo Cim.* 6 (1957) 371.
- [53] C. Itzykson, J. B. Zuber, *Quantum Field Theory*, International Series in Pure and Applied Physics, New York, USA: McGraw-Hill (1980) 705 p., 1980.
- [54] D. Binosi, A. Quadri, *Phys. Rev. D* 88 (2013) 085036.
- [55] C. Becchi, A. Rouet, R. Stora, *Annals Phys.* 98 (1976) 287–321.
- [56] I. V. Tyutin, *LEBEDEV-75-39* (1975).
- [57] L. von Smekal, R. Alkofer, A. Hauck, *Phys. Rev. Lett.* 79 (1997) 3591–3594.
- [58] C. S. Fischer, R. Alkofer, *Phys. Rev. D* 67 (2003) 094020.
- [59] J. C. R. Bloch, A. Cucchieri, K. Langfeld, T. Mendes, *Nucl. Phys. B* 687 (2004) 76–100.
- [60] O. Oliveira, P. Silva, *Braz. J. Phys.* 37 (2007) 201–207.
- [61] A. Sternbeck, K. Maltman, L. von Smekal, A. Williams, E. Ilgenfritz, M. Muller-Preussker, *PoS LATTICE2007* (2007) 256.
- [62] P. Boucaud, F. De Soto, J. Leroy, A. Le Yaouanc, J. Micheli, et al., *Phys. Rev. D* 79 (2009) 014508.
- [63] J. Horak, J. M. Pawłowski, J. Turnwald, J. M. Urban, N. Wink, S. Zafeiropoulos, *Phys. Rev. D* 107 (2023) 076019.
- [64] A. K. Cyrol, M. Mitter, J. M. Pawłowski, N. Strodthoff, *Phys. Rev. D* 97 (2018) 054006.
- [65] L. Corell, A. K. Cyrol, M. Mitter, J. M. Pawłowski, N. Strodthoff, *SciPost Phys.* 5 (2018) 066.
- [66] A. Deur, S. J. Brodsky, C. D. Roberts, *Prog. Part. Nucl. Phys.* 134 (2024) 104081.
- [67] G. F. de Teramond, A. Paul, S. J. Brodsky, A. Deur, H. G. Dosch, T. Liu, R. S. Sufian, arXiv:2403.16126 [hep-ph].
- [68] J. M. Cornwall, *Phys. Rev. D* 26 (1982) 1453.
- [69] A. C. Aguilar, J. Papavassiliou, *Nucl. Phys. Proc. Suppl.* 199 (2010) 172–177.
- [70] A. C. Aguilar, D. Binosi, J. Papavassiliou, *J. High Energy Phys.* 07 (2010) 002.
- [71] P. Boucaud, D. Dudal, J. Leroy, O. Pene, J. Rodríguez-Quintero, *J. High Energy Phys.* 12 (2011) 018.
- [72] L. von Smekal, K. Maltman, A. Sternbeck, *Phys. Lett. B* 681 (2009) 336–342.
- [73] A. C. Aguilar, D. Binosi, J. Papavassiliou, *J. High Energy Phys.* 11 (2009) 066.
- [74] E.-M. Ilgenfritz, M. Muller-Preussker, A. Sternbeck, A. Schiller, I. Bogolubsky, *Braz. J. Phys.* 37 (2007) 193–200.
- [75] I. Bogolubsky, E. Ilgenfritz, M. Muller-Preussker, A. Sternbeck, *PoS LATTICE2007* (2007) 290.
- [76] A. Cucchieri, T. Mendes, *PoS LATTICE2007* (2007) 297.
- [77] O. Oliveira, P. J. Silva, *Phys. Rev. D* 86 (2012) 114513.
- [78] J. Braun, H. Gies, J. M. Pawłowski, *Phys. Lett. B* 684 (2010) 262–267.
- [79] C. S. Fischer, A. Maas, J. M. Pawłowski, *Annals Phys.* 324 (2009) 2408–2437.
- [80] P. J. Silva, O. Oliveira, *Nucl. Phys.* (2004) 177.
- [81] H. Suman, K. Schilling, *Phys. Lett. B* 373 (1996) 314–318.
- [82] A. Cucchieri, D. Dudal, T. Mendes, O. Oliveira, M. Roelfs, P. J. Silva, *Phys. Rev. D* 98 (2018) 091504.
- [83] C. T. H. Davies, G. G. Batrouni, G. R. Katz, A. S. Kronfeld, G. P. Lepage, K. G. Wilson, P. Rossi, B. Svetitsky, *Phys. Rev. D* 37 (1988) 1581.
- [84] R. Barrett, M. Berry, T. F. Chan, J. Demmel, J. Donato, J. Dongarra, V. Eijkhout, R. Pozo, C. Romine, H. van der Vorst, *Templates for the Solution of Linear Systems: Building Blocks for Iterative Methods*, Society for Industrial and Applied Mathematics, 1994.
- [85] K. G. Wilson, *Phys. Rev. D* 10 (1974) 2445–2459.
- [86] S. Necco, R. Sommer, *Nucl. Phys. B* 622 (2002) 328–346.
- [87] P. Boucaud, F. De Soto, K. Raya, J. Rodríguez-Quintero, S. Zafeiropoulos, *Phys. Rev. D* 98 (2018) 114515.
- [88] A. G. Duarte, O. Oliveira, P. J. Silva, *Phys. Rev. D* 94 (2016) 014502.
- [89] R. G. Edwards, B. Joo (SciDAC, LHPC, UKQCD), *Nucl. Phys. B Proc. Suppl.* 140 (2005) 832.
- [90] M. Pippig, *SIAM Journal on Scientific Computing* 35 (2013) C213–C236.
- [91] O. Oliveira, P. J. Silva, J.-I. Skullerud, A. Sternbeck, *Phys. Rev. D* 99 (2019) 094506.
- [92] A. Kızılersü, O. Oliveira, P. J. Silva, J.-I. Skullerud, A. Sternbeck, *Phys. Rev. D* 103 (2021) 114515.
- [93] D. Binosi, C. D. Roberts, J. Rodríguez-Quintero, *Phys. Rev. D* 95 (2017) 114009.
- [94] D. Dudal, O. Oliveira, P. J. Silva, *Annals Phys.* 397 (2018) 351–364.
- [95] M. N. Ferreira, J. Papavassiliou, *Particles* 6 (2023) 312–363.
- [96] A. C. Aguilar, F. De Soto, M. N. Ferreira, J. Papavassiliou, J. Rodríguez-Quintero, S. Zafeiropoulos, *Eur. Phys. J. C* 80 (2020) 154.